LA-UR-11-10499
Approved for public release; distribution is unlimited.

Title: Spatially-Variant Tikhonov Regularization for Double-Difference Waveform Inversion

Author(s): Lin, Youzuo
Huang, Lianjie
Zhang, Zhigang

Intended for: 10th Annual Conference on Carbon Capture & Sequestration, 2011-05-02/2011-05-05 (Pittsburgh, Pennsylvania, United States)

CONFERENCE PROCEEDINGS

Spatially-Variant Tikhonov Regularization for Double-Difference Waveform Inversion

Youzuo Lin, Zhigang Zhang, and Lianjie Huang

TENTH ANNUAL CONFERENCE ON CARBON CAPTURE AND SEQUESTRATION - May 2-5, 2011

Spatially-Variant Tikhonov Regularization for Double-Difference Waveform Inversion

Youzuo Lin, Zhigang Zhang, and Lianjie Huang
Los Alamos National Laboratory
Geophysics Group, MS D443
Los Alamos, NM 87545

Abstract

Double-difference waveform inversion is a potential tool for quantitative monitoring for geologic carbon storage. It jointly inverts time-lapse seismic data for changes in reservoir geophysical properties. Due to the ill-posedness of waveform inversion, it is a great challenge to obtain reservoir changes accurately and efficiently, particularly when using time-lapse seismic reflection data. Regularization techniques can be utilized to address the issue of ill-posedness. The regularization parameter controls the smoothness of inversion results. A constant regularization parameter is normally used in waveform inversion, and an optimal regularization parameter has to be selected. The resulting inversion results are a trade off among regions with different smoothness or noise levels; therefore the images are either over regularized in some regions while under regularized in the others. In this paper, we employ a spatially-variant parameter in the Tikhonov regularization scheme used in double-difference waveform tomography to improve the inversion accuracy and robustness. We compare the results obtained using a spatially-variant parameter with those obtained using a constant regularization parameter and those produced without any regularization. We observe that, utilizing a spatially-variant regularization scheme, the target regions are well reconstructed while the noise is reduced in the other regions. We show that the spatially-variant regularization scheme provides the flexibility to regularize local regions based on the *a priori* information without increasing computational costs and the computer memory requirement.

1 Introduction

Monitoring changes of CO_2 reservoirs using time-lapse seismic data will play a crucial role for ensuring safe, long-term storage of carbon dioxide in geologic formations. Conventionally, reservoir changes are obtained from differences of independent inversions time-lapse data. Full-waveform inversion can be implemented in both the time domain (Tarantola 1984; Mora 1987) and the frequency domain (Pratt et al. 1998; Sirgue and Pratt 2004). In recent years, many new full-waveform inversion schemes were developed based on regularization (Hu et al. 2009; Burstedde and Ghattas 2009; Ramirez and Lewis 2010), *a priori* information (Ma et al. 2010), preconditioning (Guitton and Ayeni 2010; Tang and Lee 2010) and dimensionality reduction (Moghaddam and Herrmann 2010). Images of the conventional approach for time-lapse seismic data usually contain significant noise and artifacts. Watanabe et al. (2004) proposed a differential waveform tomography method in the frequency domain for time-lapse crosswell seismic data, and clearly showed its improvement compared to the conventional method. Denli and Huang (2009) introduced a double-difference elastic-waveform tomography method in the time domain for time-lapse surface seismic reflection data. These methods jointly invert time-lapse seismic data for reservoir changes.

To improve the robustness of double-difference waveform inversion, we develop a spatially-variant Tikhonov regularization scheme in combination with *a priori* information on space. Regularization technique is often used in inverse problems (Vogel 2002; Tarantola 2005). The most often used regularization

methods are L_2 norm based regularization (Tikhonov) and L_1 norm based regularization (total variation or compressive sensing). The spatially-variant regularization can improve inversion results for medical imaging, image restoration and other applications (Strong 1997; Guo and Huang 2009). We explore the use of the spatially-variant Tikhonov regularization scheme in double-difference full-waveform inversion. We solve the minimization of the misfit function using the block coordinate descent (BCD) scheme (Bertsekas 1999) in combination with the nonlinear conjugate gradient (NCG) approach (Nocedal and Wright 2000). The gradient of the misfit function is obtained using an adjoint method (Tarantola 1984; Tromp et al. 2005). We use a synthetic time-lapse model to verify the advantages of the spatially-variant regularization scheme for double-difference waveform inversion, and demonstrate that our new method can produce more accurate results of reservoir changes compared to those obtained using a constant regularization parameter.

2 Theory

2.1 Full-Waveform Inversion

2.1.1 Forward and Inverse Problems

The acoustic-wave equation in the time-domain is given by

$$\left[\frac{1}{K(\mathbf{r})}\frac{\partial^2}{\partial t^2} - \nabla\cdot\left(\frac{1}{\rho(\mathbf{r})}\,\nabla\right)\right] p(\mathbf{r},t) = s(t), \tag{1}$$

where $\rho(\mathbf{r})$ is the density, $K(\mathbf{r})$ is the bulk modulus, $s(t)$ is the source term, and $p(\mathbf{r},t)$ is the pressure field. The solution to (1), which is usually termed as forward modeling, is

$$\mathbf{p} = f(\mathbf{K},\boldsymbol{\rho},\mathbf{s}), \tag{2}$$

where the function of f is a given nonlinear operator. Numerical techniques such as finite difference and spectral element methods can be used to solve (2). Let the model parameter be

$$\mathbf{m} = \begin{bmatrix}\mathbf{K}\\ \boldsymbol{\rho}\\ \mathbf{s}\end{bmatrix},$$

we can rewrite (2) as

$$\mathbf{p} = f(\mathbf{m}). \tag{3}$$

The inverse problem of equation (3) is usually posed as a minimization problem such that

$$E(\mathbf{m}) = \min_{\mathbf{m}}\left\{||\mathbf{p} - f(\mathbf{m})||_2^2\right\}, \tag{4}$$

where $E(\mathbf{m})$ is the misfit function, and $||\cdot||_2$ stands the L_2 norm. In the inverse problem, $\mathbf{p}$ corresponds to observed waveforms. The minimization of (4) is to find a model $\mathbf{m}$ that yields the minimum difference between observed and synthetic waveforms.

2.2 Double-Difference Waveform Inversion

Conventionally, two independent inversions in (4) are carried out to obtain the time-lapse changes in reservoir, that is

$$\delta\mathbf{m}_{\mathrm{conv}} = f^{-1}(\mathbf{p}_{\mathrm{time\ 2}}) - f^{-1}(\mathbf{p}_{\mathrm{time\ 1}}), \tag{5}$$

where f^{-1} means the general inverse of waveform data, and $\mathbf{p}_{\mathrm{time\ 1}}$ and $\mathbf{p}_{\mathrm{time\ 2}}$ are data collected at two different times.

For double-difference waveform inversion, the data misfit in the cost function is replaced by

$$\delta d \equiv (\mathbf{p}_{\text{time 2}} - \mathbf{p}_{\text{time 1}}) - (\mathbf{p}_{\text{sim\_time 2}} - \mathbf{p}_{\text{sim\_time 1}}), \tag{6}$$

where the first term is the time-lapse difference in data, and the second term is the difference in synthetic time-lapse data. The method uses time-lapse seismic data to jointly invert for changes in reservoir geophysical properties.

3 *A Priori* Information and Spatially-Variant Regularization

3.1 The Roles of *A Priori* Information

A priori information plays an important role in the inverse problems. The usage of *a priori* information is usually to avoid the instability during the inversion of data (Tarantola 1984). It can be some reasonable initial guess of the solution, the smoothness of the desired reconstruction or the spatial information on the solution. In general, the *a priori* information is functioning as a guide to the true solution. More details on the effects of *a priori* information to inverse problem can be referred to (Hansen 1998; Vogel 2002; Tarantola 2005). In our work, we utilize both the spatial information and smoothness of the desired model as our *a prior* information.

There are different methods to incorporate the *a prior* information into inversion algorithms (Ma et al. 2010). We use a regularization technique in combination with the *a prior* information.

3.2 Spatially-Variant Regularization

Tikhonov regularization is a well-known technique for ill-posed problems, which is posed as a non-constrained minimization problem,

$$E(\mathbf{m}) = \min_{\mathbf{m}} \left\{ \| \mathbf{p} - f(\mathbf{m}) \|_2^2 + \lambda \| L\mathbf{m} \|_2^2 \right\} \text{ with } \lambda > 0, \tag{7}$$

where λ is the regularization parameter and L is the regularization matrix. Another equivalent form of Tikhonov regularization is given as a constrained minimization problem (Egger et al. 2006; Modarresi 2007, Section 1.2), that is,

$$\begin{aligned} &\min_{\mathbf{m}} \left\{ \| \mathbf{p} - f(\mathbf{m}) \|_2^2 \right\} \\ &\text{subject to } \| L\mathbf{m} \|_2^2 \leq \epsilon, \end{aligned} \tag{8}$$

where the parameter ϵ plays the same role as λ in (7) to control the degree of smoothness of the desired Tikhonov solution.

To incorporate the spatial information into (8), we modify (8) as

$$\begin{aligned} &\min_{\mathbf{m}} \left\{ \| \mathbf{p} - f(\mathbf{m}) \|_2^2 \right\} \\ &\text{subject to } \| L\mathbf{m}_i \|_2^2 \leq \epsilon_i, \ \mathbf{m}_i \in \Omega_i, \end{aligned} \tag{9}$$

where Ω_i is a spatial region, and ϵ_i is a spatially-variant parameter.

To incorporate the initial model, equation (9) is modified as

$$\begin{aligned} &\min_{\mathbf{m}} \left\{ \| \mathbf{p} - f(\mathbf{m}) \|_2^2 \right\} \\ &\text{subject to } \| L[\mathbf{m}_i - (\mathbf{m_0})_i] \|_2^2 \leq \epsilon_i, \ \mathbf{m}_i \in \Omega_i, \end{aligned} \tag{10}$$

where $\mathbf{m_0}$ is the initial model. The *a priori* information about the spatial characteristics of the model is used to determine spatial regions Ω_i.

3.3 How to Obtain the *A Priori* Information?

For the inverse problem based on equation (10), we need to know both the initial model $\mathbf{m_0}$ and spatial regions Ω_i. The starting model $\mathbf{m_0}$ may be obtained from ray tomography. Waveform inversion consists of two parts: migration and tomography (Mora 1989). Migration yields the shapes (or edges) of the anomalies and can be obtained in the first a few iterations during inversion. Therefore, migration results can provide the information about the spatial regions Ω_i. For double-difference waveform inversion, the target monitoring regions are the *a priori* information to be used.

4 Numerical Algorithm and Implementation

Equation (10) is the object function for our spatially-variant regularization scheme. It can be solved by converting it into an equivalent non-constrained expression. Using the Lagrange multiplier (Nocedal and Wright 2000), we have

$$E(\mathbf{m}) = \min_{\mathbf{m}} \left\{ \parallel \mathbf{p} - f(\mathbf{m}) \parallel_2^2 + \sum_i \lambda_i \parallel L[\mathbf{m}_i - (\mathbf{m_0})_i] \parallel_2^2 \right\}, \quad \text{with } \lambda_i > 0, \text{ and } \mathbf{m}_i \in \Omega_i. \tag{11}$$

The role of λ_i's is the same as ϵ_i's in (10) to control the smoothness of the reconstruction. Golub (1973) described how to compute λ for a given ϵ.

We employ a nonlinear conjugate gradient (NCG) based line search approach (Nocedal and Wright 2000) to solve equation (11). The gradient of equation (11) varies for different spatial regions. We use the block coordinate descent (BCD) approach that has been proved to be quite efficient for such a situation (Bertsekas 1999; Wu and Lange 2008; Li and Osher 2009).

4.1 Block Coordinate Descent

Analogous to the Gauss-Seidel matrix solver algorithm in optimization, BCD partitions the coordinates into N blocks, and improves the estimation of the solution in each block by minimizing along one direction with all the other blocks fixed. The order in which the blocks are visited is called "sweep pattern." The order of the blocks visited does matter in BCD algorithm. In our algorithm, we use a "cyclic pattern," which means all the blocks are visited sequentially. It has been illustrated that using different visiting orders may help in improving the convergence rate of the algorithms (Wu and Lange 2008; Li and Osher 2009).

To ensure the convergence as in the line search algorithm, the search direction $\mathbf{d}_k$ along each block needs to be a descent direction. In the other words, for the function $E(\mathbf{m})$, $\mathbf{d}_k$ needs to satisfy

$$cos\,\theta = \frac{\nabla E_k^T \mathbf{d}_k}{||\nabla E_k||\ ||\mathbf{d}_k||} \ < \ 0, \tag{12}$$

where θ is the angle between the search direction and ∇E_k. We use the conjugate-gradient direction as the search direction for each block.

After obtaining the search direction for a particular block, the line search with the Armijo criteria is further utilized for the optimal step size. We then update the block with the search direction and its step size without affecting other blocks:

$$\mathbf{m}_i^{(k+1)} = \mathbf{m}_i^{(k)} + \alpha_i^{(k)} \mathbf{d}_i^{(k)}, \tag{13}$$

where the superscripts stands for the iteration number and the subscript stands for the block index.

4.2 Nonlinear Conjugate Gradient

The search directions in BCD are calculated from nonlinear conjugate gradients, as illustrated in Nocedal and Wright (2000). The method to incorporate BCD with NCG is to replace the updating step (step 3) in Algorithm 1 with (13).

Algorithm 1 Canonical NCG to solve $\min_{\mathbf{m}} E(\mathbf{m})$

Input: $\mathbf{m}^{(0)}$, TOL
Output: $\mathbf{m}^{(k)}$

1: Initialize $k = 0$, $E^{(0)} = E(\mathbf{m}^{(0)})$, $\nabla E^{(0)} = \nabla E(\mathbf{m}^{(0)})$;
2: **while** $||\nabla E^{(k)}|| > \text{TOL}$ **do**
3: Compute $\alpha^{(k)}$ and update the solution $\mathbf{m}^{(k+1)} = \mathbf{m}^{(k)} + \alpha^{(k)}\mathbf{d}^{(k)}$;
4: Evaluate $\nabla E^{(k+1)}$;
5: $\beta^{(k+1)} = \frac{<\nabla E^{(k+1)}, \nabla E^{(k+1)}>}{<\nabla E^{(k)}, \nabla E^{(k)}>}$;
6: $\mathbf{d}^{(k+1)} = -\nabla E^{(k+1)} + \beta^{(k+1)}\mathbf{d}^{(k)}$;
7: $k \longleftarrow k + 1$;
8: **end while**

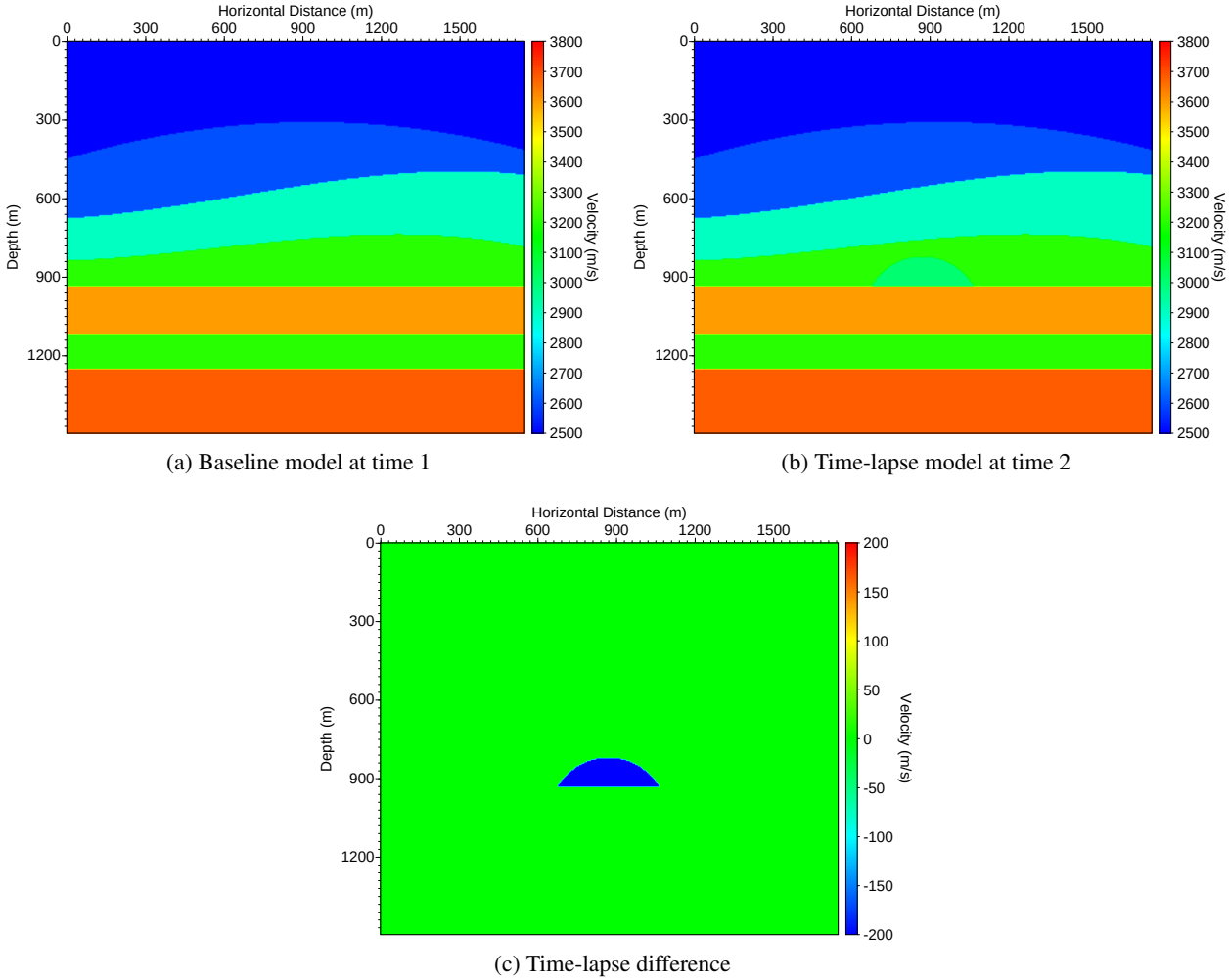

(a) Baseline model at time 1

(b) Time-lapse model at time 2

(c) Time-lapse difference

Figure 1: The baseline velocity model (a) and the time-lapse velocity model (b) that contains a region with a decreased velocity shown in (c) due to CO_2 injection.

5 Numerical Results

We use synthetic time-lapse surface seismic data for the models in Fig. 1 to demonstrate the improvement of the double-difference waveform inversion with a spatially-variant Tikhonov regularization scheme. There is a region in Fig. 1b with a decreased velocity due to CO_2 injection and migration, as shown in Fig. 1c. Five

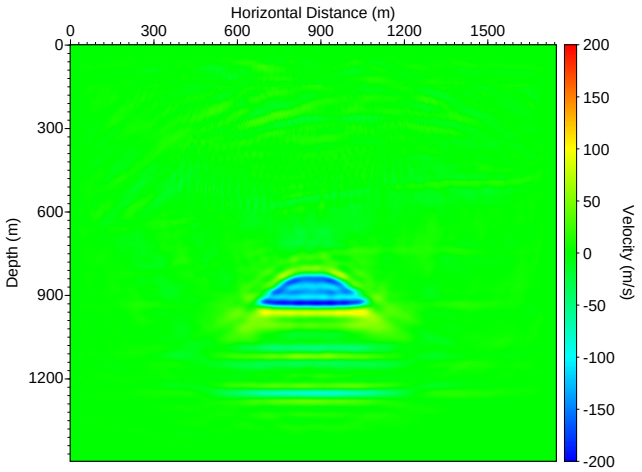

(a) The difference of two independent inversions

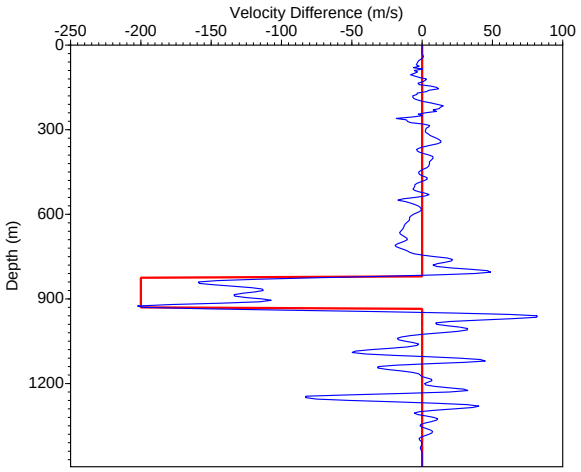

(b) A vertical profile of the result in (a)

Figure 2: The difference (a) of two independent inversions of synthetic time-lapse seismic data for the models in Fig. 1 together with a vertical profile (b) at the horizontal position of 875 m of the result in (a). The red line in (b) shows the true velocity change, and the blue line is the difference of two independent inversions.

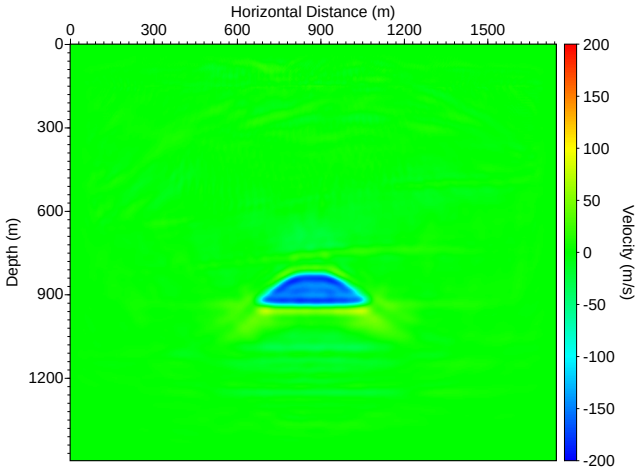

(a) Reconstructed velocity difference

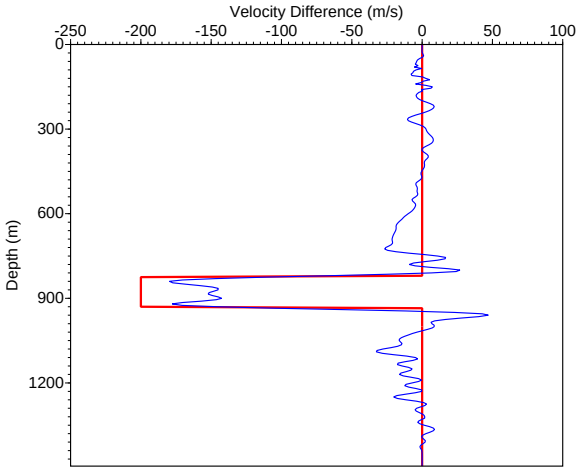

(b) A vertical profile of the result in (a)

Figure 3: The result of double-difference waveform inversion with a constant regularization parameter $\lambda = 1.0 \times 10^{-13}$ together with a vertical profile at the horizontal position of 875 m. The red line in (b) shows the true velocity change, and the blue line is the result of double-difference waveform inversion with a constant regularization parameter.

common-shot gathers of synthetic time-lapse seismic data with 350 receivers at the top of the models are used to jointly invert for the reservoir change. The shot interval is 300 m and the receiver interval is 5 m. A Ricker's wavelet with a center frequency 25 Hz is used as the source function.

For comparison, we first obtain the velocity change in the target monitoring region using the conventional approach by subtracting the two independent inversions and using the double-difference waveform inversion with a constant regularization parameter. The result of the conventional approach in Fig. 2 contains significant image artifacts. The vertical profile in Fig. 2b shows that the reconstructed velocity change in the target region is approximately -120 m/s, significant different from the true value of -200 m/s. In addition, it contains significant image noise above and below the target monitoring region.

Figure 3 shows the result of double-difference waveform inversion with a constant regularization parameter $\lambda = 1.0 \times 10^{-13}$. The reconstructed velocity change in the target region is approximately -165 m/s,

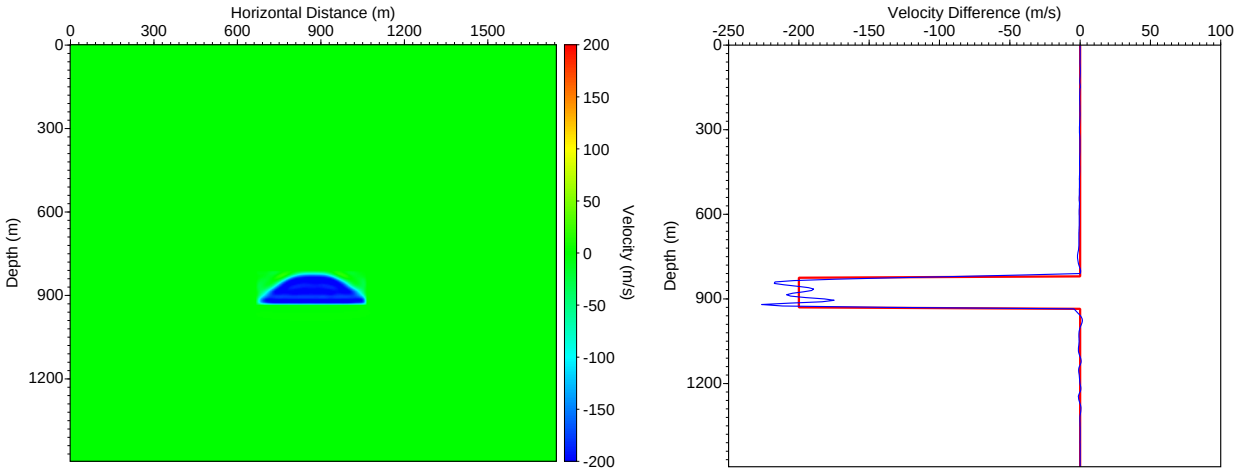

(a) Reconstructed velocity difference

(b) A vertical profile of the result in (a)

Figure 4: The result of double-difference waveform inversion with a spatially-variant regularization parameter together with a vertical profile at the horizontal position of 875 m. The red line in (b) shows the true velocity change, and the blue line is the result of double-difference waveform inversion with spatially-variant Tikhonov regularization.

which is closer to the true value of -200 m/s compared to that obtained using the conventional approach. Figure 3 contain fewer noise than Fig. 2.

In order to incorporate the *a priori* spatial information into the spatially-variant Tikhonov regularization scheme for double-difference waveform inversion, we determine the target monitoring regions using the result of the first a few iterations. There are two regions in equation (11) for our time-lapse models in Fig.1, one within the target monitoring region, and the other outside the target monitoring region. The regularization parameter utilized for the target monitoring region is $\lambda_{in} = 1.0 \times 10^{-13}$, and $\lambda_{out} = 1.0 \times 10^{-10}$ for the other region. Figure 4 shows the result of double-difference waveform inversion with a spatially-variant regularization parameter. The reconstructed velocity change in the target monitoring region is approximately -200 m/s. Figure 4 contains significant fewer image artifacts outside the target monitoring region compared to Fig. 2 and Fig. 3.

The computational cost of the double-difference waveform inversion with a spatially-variant Tikhonov regularization parameter is comparable to that with a constant regularization parameter.

6 Conclusions

We have developed a spatially-variant Tikhonov regularization scheme for double-difference waveform inversion. The method employs different regularization parameters in different regions in space. It uses the block coordinate descent and nonlinear conjugate gradient schemes. Our results of synthetic time-lapse seismic data demonstrate that our new method can reconstruct accurate values of velocity changes due to CO_2 injection, and produce images of reservoir changes with much fewer image artifacts than those obtained using double-difference waveform inversion with a constant regularization parameter.

Acknowledgement

This work was supported by the U.S. Department of Energy and managed by the National Energy Technology Laboratory through contract DE-AC52-06NA25396 to Los Alamos National Laboratory.

References

Bertsekas, D. P., 1999, Nonlinear programming: Athena Scientific.

Burstedde, C., and O. Ghattas, 2009, Algorithmic strategies for full waveform inversion: 1d experiments: Geophysics, **74**, 37–46.

Denli, H., and L. Huang, 2009, Double-difference elastic waveform tomography in the time domain: 79th Annual International Meeting, SEG, Expanded Abstracts, 2302–2306.

Egger, H., T. Hein, and B. Hofmann, 2006, On decoupling of volatility smile and term structure in inverse option pricing: Inverse Problem, **22**, 1247–1259.

Golub, G. H., 1973, Some modified matrix eigenvalue problems: SIAM Review, **15**, 318–334.

Guitton, A., and G. Ayeni, 2010, A preconditioning scheme for full waveform inversion: 80th Annual International Meeting, SEG, Expanded Abstracts, 1008–1012.

Guo, W., and F. Huang, 2009, Adaptive total variation based filtering for MRI images with spatially inhomogeneous noise and artifacts: ISBI, 101–104.

Hansen, P. C., 1998, Rank-deficient and discrete ill-posed problems: Numerical aspects of linear inversion: SIAM.

Hu, W., A. Abubakar, and T. Habashy, 2009, Simultaneous multifrequency inversion of full-waveform seismic data: Geophysics, **74**, 1–14.

Li, Y., and S. Osher, 2009, Coordinate descent optimization for l_1 minimization with application to compressed sensing: a greedy algorithm: Inverse Problem Imaging, **3**, 487–503.

Ma, Y., D. Hale, Z. Meng, and B. Gong, 2010, Full waveform inversion with image-guided gradient: 80th Annual International Meeting, SEG, Expanded Abstracts, 1003–1007.

Modarresi, K., 2007, A local regularization method using multiple regularization levels: PhD thesis, Stanford University.

Moghaddam, P., and F. J. Herrmann, 2010, Randomized full-waveform inversion: a dimensionality-reduction approach: 80th Annual International Meeting, SEG, Expanded Abstracts, 977–982.

Mora, P., 1987, Nonlinear two-dimensional elastic inversion of multioffset seismic data: Geophysics, **54**, 1211–1228.

———, 1989, Inversion = migration + tomography: Geophysics, **54**, 1575–1586.

Nocedal, J., and S. Wright, 2000, Numerical optimization: Springer.

Pratt, R. G., C. Shin, and G. J. Hicks, 1998, Gauss-newton and full newton methods in frequency-space seismic waveform inversion: Geophysical Journal International, **13**, 341–362.

Ramirez, A., and W. Lewis, 2010, Regularization and full-waveform inversion: A two-step approach: 80th Annual International Meeting, SEG, Expanded Abstracts, 2773–2778.

Sirgue, L., and R. G. Pratt, 2004, Efficient waveform inversion and imaging: A strategy for selecting temporal frequency: Geophysics, **69**, 231–248.

Strong, D., 1997, Adaptive total variation minimizing image restoration: PhD thesis, University of California at Los Angeles.

Tang, Y., and S. Lee, 2010, Preconditioning full waveform inversion with phase-encoded hessian: 80th Annual International Meeting, SEG, Expanded Abstracts, 1034–1038.

Tarantola, A., 1984, Inversion of seismic reflection data in the acoustic approximation: Geophysics, **49**, 1259–1266.

———, 2005, Inverse problem theory: SIAM.

Tromp, J., C. Tape, and Q. Liu, 2005, Seismic tomography, adjoint methods, time reversal and banana-doughnut kernels: Geophysical Journal International, **160**, 195–216.

Vogel, C., 2002, Computational methods for inverse problems: SIAM.

Watanabe, T., S. Shimizu, E. Asakawa, and T. Matsuoka, 2004, Differential waveform tomography for time-lapse crosswell seismic data with application to gas hydrate production monitoring: 74th Annual International Meeting, SEG, Expanded Abstracts, 2323–2326.

Wu, T., and K. Lange, 2008, Coordinate descent algorithm for lasso penalized regression: The Annals of Applied Statistics, **2**, 224–244.